*Electronic Supporting Information (ESI) of*

# Time Evolution of Moduli of a Polymer-Induced Liquid-Precursor (PILP) of Calcium Carbonate

*Changyu Shao,[a,b,f] Haihua Pan,*[b] Jinhui Tao,[c] Kang Rae Cho,[d,e] Ruikang Tang,*[f] Laurie B. Gower,[g] and James J. De Yoreo*[c]*

*[a] Stomatology Hospital, School of Stomatology, Zhejiang University School of Medicine, Clinical Research Center for Oral Diseases of Zhejiang Province, Key Laboratory of Oral Biomedical Research of Zhejiang Province, Cancer Center of Zhejiang University, Hangzhou, 310006, China*
*[b] Qiushi Academy for Advanced Studies, Zhejiang University, Hangzhou, 310027, China*
*[c] Physical Sciences Division, Pacific Northwest National Laboratory, WA, 99354,USA*
*[d] Molecular Foundry, Lawrence Berkeley National Laboratory,CA, 94720, USA*
*[e] Department of Applied Chemistry, College of Engineering, Cheongju University, Cheongju 28503, Republic of Korea*
*[f] Centre for Biomaterials and Biopathways and Department of Chemistry, Zhejiang University, Hangzhou, 310027, China*
*[g] Department of Materials Science & Engineering, University of Florida,FL 32611-6400, USA*

## Contents

1. Experimental Section

2. Supported Figures

3. Supported Text

4. References

# 1.Experimental section

## 1.1 Materials

All chemicals were purchased from Sigma-Aldrich (St Louis, MO, USA) unless specifically mentioned. Poly(acrylic acid sodium salt) of 5100 g/mol (PAA-5k). De-ionized Milli-Q water (Millipore Milli-Q, Bedford, MA, USA) was used and all solutions were filtered through 0.22 μm Millipore films prior to use.

## 1.2. Mineralization solutions

Calcium solution: 30 mM $CaCl_2$; Bicarbonate solution: 30 mM $NaHCO_3$, 40 μg/mL PAA-5k; PILPs were freshly prepared by mixing calcium and bicarbonate solutions (1:1 by volume). The pH was about 8 after mixing. Immediately after mixing the calcium and bicarbonate solutions, a 20 μL aliquot was deposited on a silicon wafer and precipitation was observed under an optical microscope. In ambient open-air conditions (25 °C and 60% relative humidity), we found that a mineral “film” was precipitated at the rim of the drop (i.e. the solution-air-silicon interface) (see Fig. S1a), presumably due to the increase of supersaturation as $CO_2$ was released. SEM imaging shows that the film-like precipitate seen optically (Fig. S1a) was actually composed of agglomerated structures exhibiting a distinctly liquid-like morphology (Fig. S1b and c), consistent with previous findings of PILP behavior. The morphologies produced by precipitates that had partially merged were strikingly reminiscent of those formed when viscous liquid droplets partially merge together and spread on a surface. These partially coalesced droplets however did not form a continuous film, suggesting an evolution in the PILP’s mechanical properties, becoming gradually less fluidic and eventually solidifying. Upon continued aging, the precipitates finally crystallized. Micro-Raman analysis showed that the precursor phase and final crystalline phases were amorphous calcium carbonate (ACC) and vaterite, respectively (see Fig. S2).

## 1.3. In situ Atomic Force Microscopy (AFM)

Immediately after a 20 μL aliquot was deposited on a silicon wafer, it was transferred to the sample stage of the AFM and sealed in a liquid cell. About 100 μL of calcium carbonate solution was then injected to fill the liquid cell before AFM imaging. In-situ AFM images were collected at 25 °C in tapping mode with oxide-sharpened silicon nitride probes (NP-S, Veeco; k=0.5 nN/nm, f=9 kHz ) (Veeco Nanoscope IVa, USA). To reduce possible imaging artefacts, the force exerted by the tip on the surface was minimized. Force curve measurements were obtained using a procedure similar to that for imaging, except that a blunt probe was used for indentation. NP-S probes (Veeco) were milled using a FIB (Zeiss CrossBeam 1540EsB, Carl Zeiss Microscopy GmbH, Germany; 30 keV gallium beam, 50 pA) to obtain a cone tip with a diameter of 120 nm (see Scheme S1).

### 1.4. Characterizations

Samples of the precipitates from the silicon wafers were prepared by removing the solution using compressed $N_2$ gas and drying the samples in air. SEM images were taken on a Zeiss Gemini Ultra-55 (with an acceleration voltage of 1.5 kV). The phases of the precipitates were characterized by a LabRAM ARAMIS confocal Raman microscope (HORIBA scientific, Japan) operated at a resolution of 2 $cm^{-1}$ with an excitation wavelength of 532 nm. For in situ FTIR measurement, after mixing of calcium and bicarbonate solutions (5 mL), the FTIR fiber-optic probe (Bruker Optik GmbH, Matrix-MX, Ettlingen, Germany; operated at a resolution of 4 $cm^{-1}$ and scanning from 800-2000 $cm^{-1}$, and one scan per four minutes; the first scan is used as the background to subtract out the water peak) was inserted into the solutions.

## 2. Supported Figures

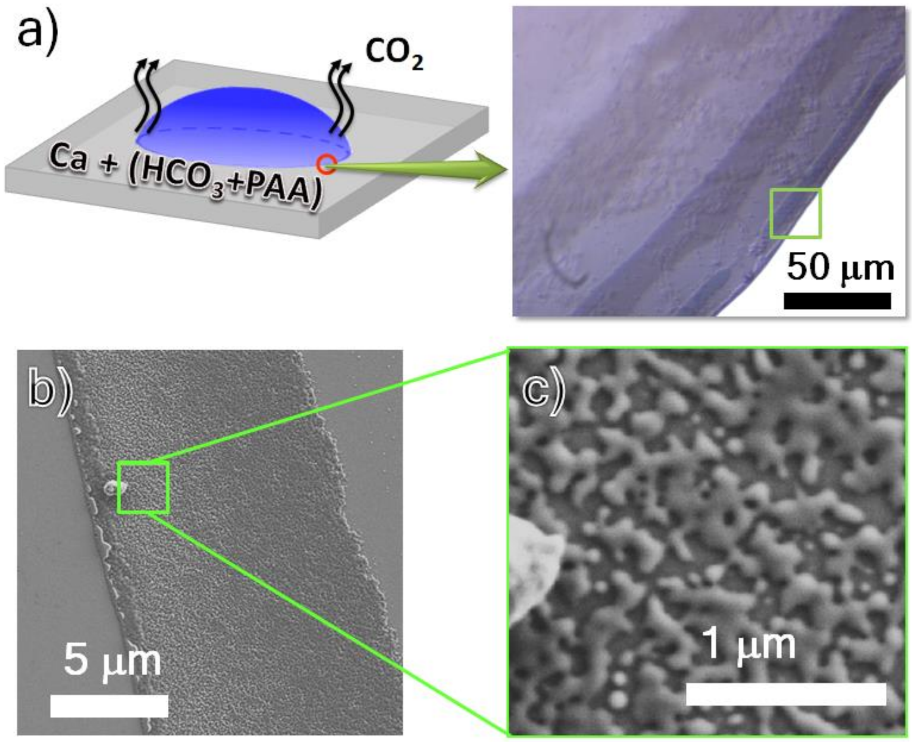

**Fig. S1** Formation of PILP in open-air. a) Schematic of PILP formation during the release of $CO_2$ and the optical image showing the precipitates near the droplet rim. b) and c) SEM images of PILP showing agglomerated patterns of droplets, which had partially merged and exhibited characteristics strikingly reminiscent of those formed when viscous liquid droplets together and on a surface.

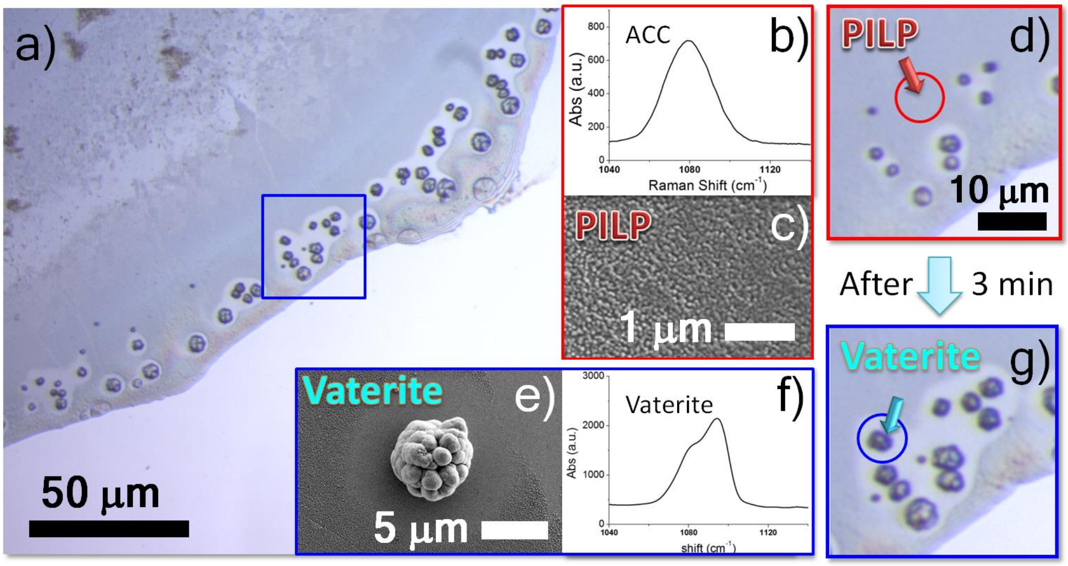

**Fig. S2** The crystallization of vaterite from PILP. a) Optical microscopy image. b) micro-Raman spectra of PILP. c) SEM image of PILP. d) and g) optical microscopy images showing PILP is dissolved as vaterite grows. e) SEM image of vaterite. f) micro-Raman spectra of vaterite.

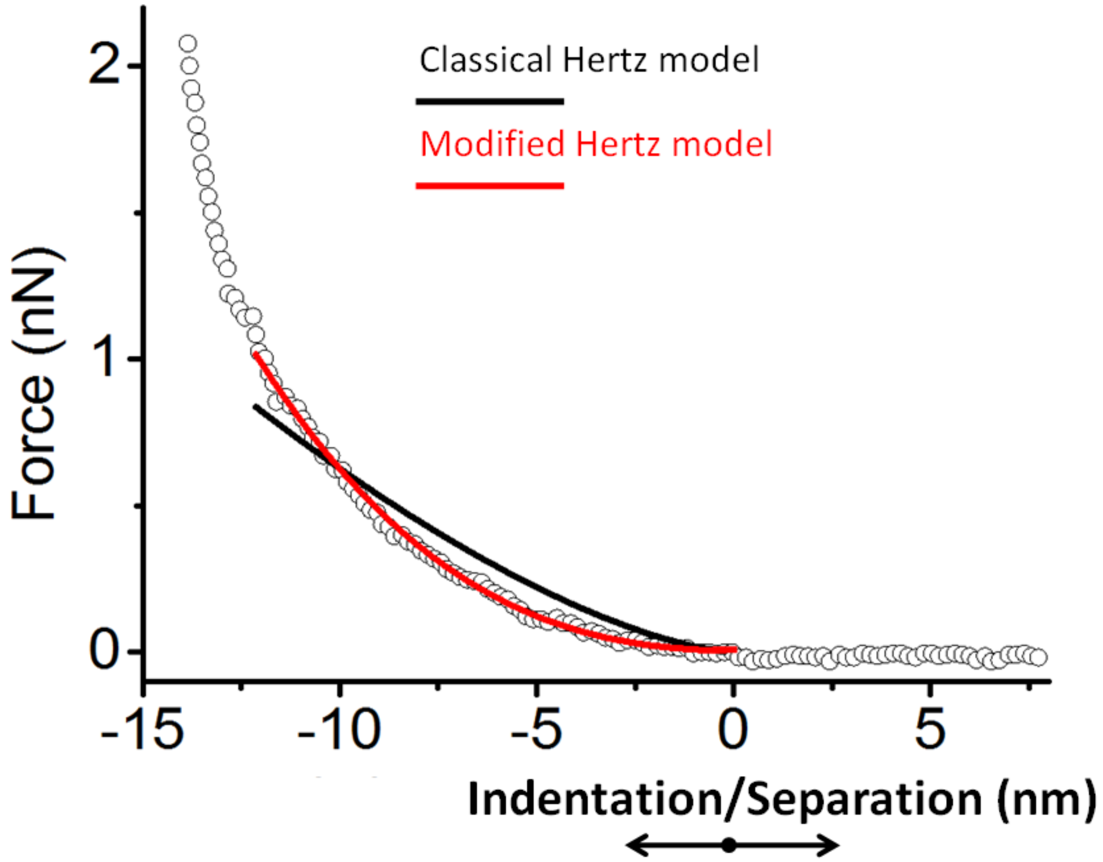

**Fig. S3** Fit to an indentation force curve using the classical Hertz (black line) and modified Hertz (red line) model. The modified Hertz model gives a better fit.

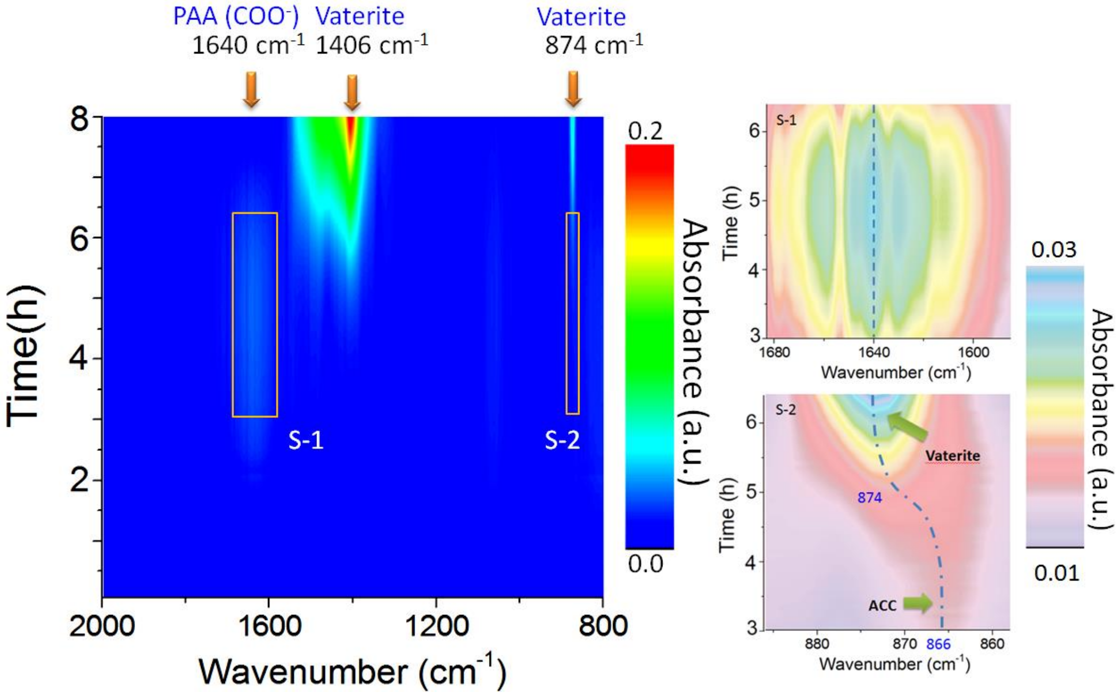

**Fig. S4** The evolution of PILP as measured by in situ FTIR. The drift of absorbance at 866 cm$^{-1}$ to 874 cm$^{-1}$ indicates the phase transformation from ACC to vaterite (see region S-2 and the zoomed-in image (lower right) in the time-resolved FTIR spectra). The appearance of the 1640 cm$^{-1}$ band (PAA COO$^{-}$) was observed for late-stage ACC (see region S-1 and the zoomed-in image in the upper right).

## 4. Supported Texts

### 1. Modified Hertz model and the Soft-stiff bilayer model

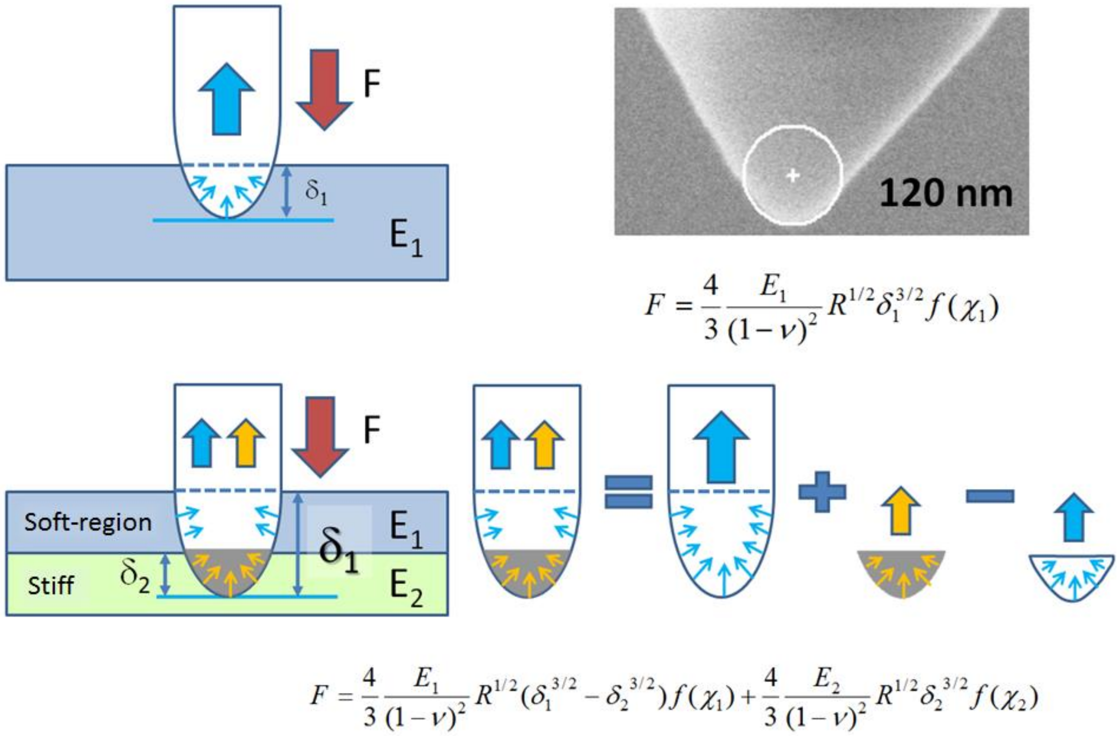

$$F=\frac{4}{3}\frac{E_1}{(1-\nu)^2}R^{1/2}\delta_1^{3/2}f(\chi_1)$$

$$F=\frac{4}{3}\frac{E_1}{(1-\nu)^2}R^{1/2}(\delta_1^{3/2}-\delta_2^{3/2})f(\chi_1)+\frac{4}{3}\frac{E_2}{(1-\nu)^2}R^{1/2}\delta_2^{3/2}f(\chi_2)$$

***Scheme S1.*** The indentation model of a soft-stiff bilayer material.

For the modified Hertz model,[S1] the indentation of a conical probe with tip radius $R$ into a thin film material (with a bulk modulus of $E$) requires a force of $F$ to indent the material to a depth of $\delta$ given by:

$$F=\frac{4}{3}\frac{E}{(1-\nu)^2}R^{1/2}\delta^{3/2}f(\chi) \quad (1)$$

where ν is Poisson’s ratio (here we take PILP to be an incompressible material, so it is about 0.5), and $f(\chi)$ is a correction factor for the stiffening effect due to finite thickness ($h$), and $\chi=\sqrt{R\delta}/h$. (In this study, $R$ = 60 nm, as shown by the SEM image of Scheme S1.) The indentation force is balanced by the counterforce acting on the cone tip (see Scheme S1 upper), so the value of the counterforce is equivalent to the indentation force, $F$.

For the indentation of a probe into a material with a soft-stiff bilayer structure, the counterforce acting on the probe can be calculated by considering the indentation force for a thin film bi-layer with different indentation depths (see Scheme S1 bottom). This indentation force is given by,

$$F = \frac{4}{3}\frac{E_1}{(1-\nu)^2}R^{1/2}(\delta_1^{\,3/2} - \delta_2^{\,3/2})f(\chi_1) + \frac{4}{3}\frac{E_2}{(1-\nu)^2}R^{1/2}\delta_2^{\,3/2}f(\chi_2) \quad (2)$$

Where the subscripts 1 and 2 indicate the upper and lower material, respectively (Scheme S1).

## 2. Droplet model

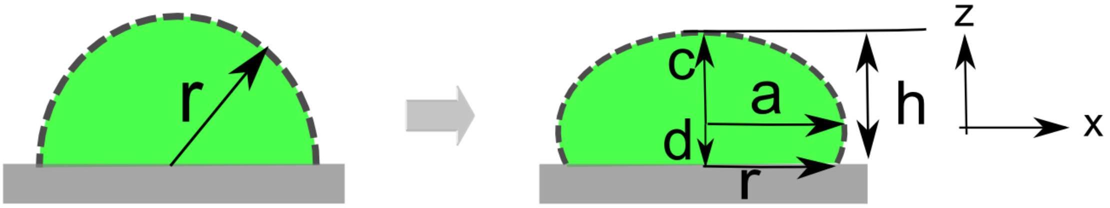

***Scheme S2.*** The deformation of PILP droplet as the push of probe during force measurements.

When pushing on a droplet with an SPM probe during force measurements, the droplet will deform, which will increase the surface area and total surface free energy. Assuming the increase of total surface free energy is given by the external work (*W*), we have,

$$W = \int F \cdot d\delta = \int \gamma \cdot \mathrm{dS} \quad (3)$$

where δ means the change in height after the pushing of an SPM probe; *F* is the force of the probe; g is the interfacial energy of the droplet, and *S* is the surface area.

Here, we assume that during the deformation, the volume is conserved and that the shape of the droplet is changed from hemi-sphere to oblate cap (see Scheme S2). That is,

$$\frac{x^2+y^2}{a^2} + \frac{z^2}{c^2} = 1 \ (4)$$

$$V = \frac{2}{3}\pi r^3 = \frac{2}{3}\pi a^2 c + \pi a^2 d\left(1 - \frac{d^2}{3c^2}\right) \ (5)$$

$$h = c + d;\ \delta = \mathrm{r} - \mathrm{h} \ (6)$$

We assume that during the deformation from a hemi-sphere to an oblate cap, the contact line of the hemi-sphere does not move. That is, $x^2 + y^2 = r^2\ when\ z = -d$. From eq. (4), we find,

$$\frac{r^2}{a^2} + \frac{d^2}{c^2} = 1 \ (7)$$

The surface area of an oblate cap is given by,

$$\mathrm{S} = \pi a \Bigg( a + d\sqrt{\frac{(a^2-c^2)d^2}{c^4} + 1} + \frac{c^2}{\sqrt{a^2-c^2}}\Bigg(\ln\left(\frac{\sqrt{a^2-c^2}+a}{c}\right) - \ln\Bigg(\sqrt{\frac{(a^2-c^2)d^2}{c^4} + 1} -$$

$$\sqrt{\frac{(a^2-c^2)d^2}{c^4}}\Bigg)\Bigg)\Bigg) = \pi r^2 \Bigg( \frac{a^2}{r^2} + \frac{a}{r}\frac{d}{r}\sqrt{\left(\frac{a^2}{c^2} - 1\right)\frac{d^2}{c^2} + 1} + \frac{\frac{ac}{rr}}{\sqrt{\frac{a^2}{c^2}-1}}\Bigg(\ln\left(\sqrt{\frac{a^2}{c^2} - 1} + \frac{a}{c}\right) -$$

$$\ln\Bigg(\sqrt{\left(\frac{a^2}{c^2}-1\right)\frac{d^2}{c^2}+1}-\sqrt{\left(\frac{a^2}{c^2}-1\right)\frac{d^2}{c^2}}\Bigg)\Bigg)\Bigg) = F\left(\frac{a}{r},\frac{c}{r},\frac{d}{r}\right) \quad (8)$$

We can get *S* once we know *a/r*, *c/r*, and *d/r*, which is a function of δ, and these can be determined by the conservation of volume (eq. 5), and the boundary conditions (eq. 7). For simplicity, we set,

$$\delta = g \cdot r,\ \left( 0 \le g \le 1 \right) \quad (9)$$

Combining (5), (6), (7), and (9) we get,

$$\left(\frac{a}{r}\right)^2 = \frac{(1+g)^2}{(1-g)(1+3g)} \quad (10)$$

$$\frac{c}{r} = \frac{(1-g)(1+g)}{1+3g} \quad (11)$$

$$\frac{d}{r} = \frac{2(1-g)g}{1+3g} \quad (12)$$

Combining (3) and (9), we get,

$$\mathrm{F} = \gamma\frac{dS}{d\delta} = \frac{\gamma}{r}\frac{dS}{dg} \quad (13)$$

Where *S* is a function of *g* (Eqs. 8, 10-12), and d*S*/d*g* can be solved numerically by using Eqs. (8, 10-12).

## 4. References

[S1] E. K. Dimitriadis, F. Horkay, J. Maresca, B. Kachar, R. S. Chadwick, *Biophys. J.* 2002, **82**, 2798-2810.